

Constructing New Biorthogonal Wavelet Type which Matched for Extracting the Iris Image Features

by R. Rizal Isnanto

Submission date: 30-Sep-2022 01:09PM (UTC+0700)

Submission ID: 1912790100

File name: Turnitin_C6.pdf (738.93K)

Word count: 4209

Character count: 21286

OPEN ACCESS

Constructing New Biorthogonal Wavelet Type which Matched for Extracting the Iris Image Features

24

To cite this article: R Rizal Isnanto *et al* 2013 *J. Phys.: Conf. Ser.* **423** 012020

View the [article online](#) for updates and enhancements.

You may also like

27

- [Dynamical scaling of Loschmidt echo in \$\phi^4\$ -Hermitian systems](#)

Jia-Chen Tang, Su-Peng Kou and Gaoyong Sun

- [Biorthogonal quantum mechanics](#)
Dorje C Brody

- [Synchronization of autonomous ultradiscrete hungry Toda lattice and a generalized box-ball system](#)
Kazuki Maeda



The Electrochemical Society
Advancing solid state & electrochemical science & technology

242nd ECS Meeting

Oct 9 – 13, 2022 • Atlanta, GA, US

Early hotel & registration pricing ends September 12

Presenting more than 2,400 technical abstracts in 50 symposia

The meeting for industry & researchers in

BATTERIES
ENERGY TECHNOLOGY
SENSORS AND MORE!

 **Register now!**



ECS Plenary Lecture featuring M. Stanley Whittingham,
Binghamton University
Nobel Laureate –
2019 Nobel Prize in Chemistry



18

Constructing New Biorthogonal Wavelet Type which Matched for Extracting the Iris Image Features

Rizal Isnanto¹, Suhardjo², Adhi Susanto³

¹Doctor Candid³ of Electrical of Electrical Engineering UGM Yogyakarta, Indonesia and ²Lecturer of Engineering Faculty, UNDIP Semarang, Indonesia

²Professor in Medicine Faculty UGM Yogyakarta

³Professor in Electrical Engineering and Information Technology Department UGM Yogyakarta

³e-mail: rizal_isnanto@undip.ac.id and rizal_isnanto@yahoo.com

Abstract. Some former research have been made for obtaining a new type of wavelet. In case of iris recognition using orthogonal or biorthogonal wavelets, it had been obtained that Haar filter is most suitable to recognize the iris image. However, designing the new wavelet should be done to find a most matched wavelet to extract the iris image features, for which we can easily apply it for identification, recognition, or authentication purposes. In this research, a new biorthogonal wavelet was designed based on Haar filter properties and Haar's orthogonality conditions. As result, it can be obtained a new biorthogonal 5/7 filter type wavelet which has a better than other types of wavelets, including Haar, to extract the iris image features based on its mean-squared error (MSE) and Euclidean distance parameters.

1. Introduction

1.1 Background

Humans as individuals, have unique characteristics and distinctive. These characteristics can be used to recognize or identify persons. This is known as biometric recognition. Iris is the part of the circle around³⁰ the pupil. Although iris has a relatively narrow region compared with entire area of the human body, iris has a very unique pattern, different in each individual and the pattern will remain stable. For those reasons, iris can be used as the basis for the recognition in biometrics.

Many algorithms have been applied as a method of iris recognition, such as ³PCA (Principal Component Analysis), ICA (Independent Compone³¹ Analysis), Gabor-Wavelet algorithm [6], characterizing Key Local Variation, Laplace Pyramid, Gray Level Co-occurrence Matrix (GLCM) [3] and others.

Wavelet transform as one method for analyzing textures has been used as iris image feature extractor. However, it is still limited applying the standard orthogonal wavelet types, for example: Haar, Daubechies, Coiflet, and Symlet. In this research, a new type of biorthogonal wavelet will be develop. Some parameters in Haar filter properties and Haar's orthogonality conditions will be applied. The length of filters are 5 (five) for decomposition and 7 (seven) for reconstruction, The notation used to come is Biorthogonal 5/7 for the upcoming filter.

To extract the iris image features, two parameters used, i.e. mean-squared error (MSE) and Euclidean distance parameters.

1.2 Research Objective

The purpose of making this research is to develop a new type of biorthogonal wavelet. Some parameters in Haar filter properties and Haar's orthogonality conditions will be applied in the design steps. The length of filters are 5 (five) for decomposition and 7 (seven) for reconstruction. The wavelet used to come is Biorthogonal 5/7 for the upcoming filter. To extract the iris image features, two parameters used, i.e. mean-squared error (MSE) and Euclidean distance parameters.

1.3 Limitations

- In order not to deviate far from the problems, then this study has problem limitations as follows:
- Iris image used is the image from database of CASIA V1.0 – Portions of the research in this paper use the CASIA-IrisV1 collected by the Chinese Academy of Sciences' Institute of Automation (CASIA) – and iris images captured using Irdosoft 4.0 camera.
 - Research uses of Haar filter parameters and its orthogonality properties as the basis for reconstructing a new 5/7 biorthogonal wavelet. The reason of using Haar parameter is that in previous research, Haar wavelet is the best wavelet for recognizing iris images based on recognition rate [9],[11] as well as based on energy compaction [10].
 - Recognition method used is the normalized Euclidean distance method

2. Basis of Theory

2.1 Iris Eyes

Iris can serve as the basis for biometric systems. Each iris has a texture that is very detailed and unique to each person and remain stable for decades. The eye can not be altered through surgery without causing any damage to eyesight. Fig.1 shows the anatomy of the eye, and examples of human iris [2].

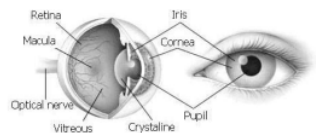


Figure 1. Anatomy of eyes and example of iris region.

The advantages of using the iris for reliable identification system are [2] as follows.

- Iris is insulated and shielded from the outside environment.
- In the iris, it is not possible to do some surgeries without causing defects in the eye.
- Iris has a physiological response to light, which allows testing of the natural use of the possibility of fraud and faked eye lenses and so forth.

2.2 Wavelet Transform

Wavelets are mathematical functions that satisfy certain requirements are able to perform the decomposition of a function [13]. Hierarchically, wavelet is used to represent data or other functions. Wavelet can be used to describe a model or the original image into a mathematical function regardless of the shape of the model in the form of image, a curve or a plane. Wavelet transform is a function that converts the signals from region to region the frequency or time scale. The most appropriate wavelet transform used in image processing because there is not much information is lost during the reconstruction.

Wavelet is a base derived from a wavelet basis function which is also said to be a scaling or scaling function. Scaling function has properties which can be assembled from a number of copies that have been dilated, translated and scaled. This function is derived from the dilation equation, which is considered as the basis of wavelet theory.

2.3 Image Decomposition

Image processing using wavelet transform is done by filtering image using wavelet filter. Result of this filtering is 4 image subspaces from original image. These four subspaces are in wavelet domain. Four subspaces mentioned are lowpass-lowpass (LL), lowpass-highpass (LH), highpass-lowpass (HL), and highpass-highpass (HH). This process is called decomposition.

The decomposition can be continued using lowpass-lowpass (LL) as its input for getting next decomposition stages. Figure 4 shows a decomposition image from level 1 until level 3. Maximum level of decomposition in image processing using wavelet (except biorthogonal wavelets) can be formulated as follows [4].

$$\text{Level}_{\max} = \frac{\log(\text{data length}/(\text{filter length} - 1))}{\log(2)} \quad (1)$$

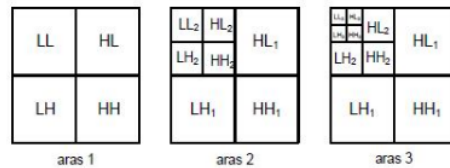


Figure 2. Diagram of image decomposition.

2.4 Normalized Euclidean Distance

After passing through feature extraction process and parameter values are obtained, then the next stage is calculating the nearest distance (Euclidean distance) of feature vector values of an image [14]. The closer the Euclidean distance, getting closer to a certain image. For example, values of feature vectors of input image $A_i = (A_1, A_2, \dots, A_n)$ and values of feature vector of j -th image is $B_j = (B_{1j}, B_{2j}, \dots, B_{nj})$, then Euclidean distance between values of feature vectors of input image and values of feature vector of j -th image can be expressed as:

$$D(A, B) = \sqrt{\sum_{i=0}^n \frac{(A_i - B_i)^2}{A_i}} \quad (2)$$

where:

$D(A, B)$ = Euclidean distance between iris A and B

A_i = Feature vector of iris A

B_i = Feature vector of iris B

n = vector length (sum of textural features) of vector A and vector B

2.5 Successive Approximation or Cascade Algorithm

One approach to calculate $\varphi(t)$ and $\psi(t)$ is a form of successive approximation that is used theoretically to prove existence and uniqueness of $\varphi(t)$ and can also be used to actually calculate them. The basic recursion equation that comes from multiresolution formulation is

$$\varphi(t) = \sum_n h[n] \sqrt{2} \varphi^{(k)}(2t - n) \quad (3)$$

where $h(n)$ is the scaling coefficients and $\varphi(t)$ is the scaling function which satisfies this equation.

In order to solve the basic recursion equation (3), an iterative algorithm that will generate successive approximations to $\psi(t)$ is applied [7]. If the algorithm converges to a fixed point, then that fixed point is a solution to (3).

The iterations are defined by

$$\varphi^{(k+1)}(t) = \sum_{n=0}^{N-1} h[n] \sqrt{2} \varphi^{(k)}(2t - n) \quad (4)$$

This iteration converges to $\varphi(t)$. From this $\varphi(t)$, then the wavelet function can be generated from

$$\psi(t) = \sum_{n=-\infty}^{\infty} g[n] \sqrt{2} \varphi^{(k)}(2t - n) \quad (5)$$

Because it applies the same operation over and over to the output of the previous application, it is known as the *cascade algorithm* [13].

2.6 Biorthogonal wavelet

A biorthogonal wavelet is a wavelet where the associated wavelet transform is invertible but not necessarily orthogonal. Designing biorthogonal wavelets allows more degrees of freedom than orthogonal wavelets. One additional degree of freedom is the possibility to construct symmetric wavelet functions.

In the biorthogonal case, there are two scaling functions $\varphi, \tilde{\varphi}$, which may generate different multiresolution analyses, and accordingly two different wavelet functions $\psi, \tilde{\psi}$. So the numbers M and N of coefficients in the scaling sequences a, \tilde{a} may differ. The scaling sequences must satisfy the following biorthogonality condition [12].

$$\sum_{n \in \mathbb{Z}} a_n \tilde{a}_{n+2m} = 2 \delta_{m,0} \quad (6)$$

Then the wavelet sequences can be determined as

$$b_n = (-1)^n \tilde{a}_{M-1-n}, n=0, \dots, M-1 \quad (7)$$

and

$$\tilde{b}_n = (-1)^n a_{M-1-n}, n=0, \dots, N-1 \quad (8)$$

3. Design of Research

In constructing a new 5/7 biorthogonal wavelet, chart to be followed is depicted in figure 3.

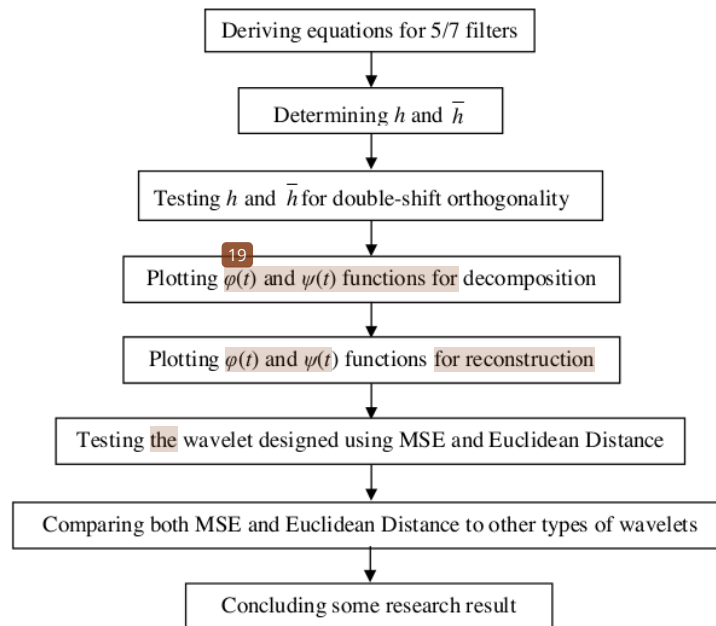


Figure 3. Chart of research design

From figure 3, it can be detailed as follows.

- Deriving and then obtaining some equations for 5-tap filters as well as for 7-tap filters which satisfies orthogonality conditions.
- Determining the components of h and \bar{h} which depicting filter components for decomposition and reconstruction, respectively.
- Testing the results of point b in case of its double-shift orthogonality.
- Plotting and depicting two graphics both scaling function as well as wavelet function for decomposition purpose using cascade algorithm applied up to 20 iterations.
- Plotting and depicting two graphics both scaling function as well as wavelet function for reconstruction purpose using cascade algorithm applied up to 20 iterations.
- Testing the wavelet designed using both MSE and Euclidean distance measures between reconstructed iris images after decomposition and its original images.
- Comparing both MSE and Euclidean distance (results from point f) against other types of wavelets which had ever observed (i.e. Haar, db5, coif3, sym4, and bior2.4).
- Concluding some results of points f and g to give research conclusions.

4. Designing the Biorthogonal Wavelet using 5/7 Filter

The meaning of 5/7 indicates that one filter which has length of 5 (five) for decomposition and 7 (seven) for reconstruction.

The reasons why we choose 5/7 biorthogonal filter are: biorthogonal wavelet bases maintain the symmetry for wavelets and scaling functions by relaxing the orthogonality constraint [15], while none of the orthogonal wavelet systems, except Haar, has symmetrical coefficients [8]. Also, the orthogonal wavelets filter and scaling filter must be of the same length, and the length must be even [7]. This

restriction has been relaxed for biorthogonal filters. Since we had done some research previously to construct Biorthogonal 2/6 and 3/5 filters [15] to represent short-medium length filters, then we choose Biorthogonal 5/7 as a representative of a relatively medium-medium filters with odd lengths both for analysis and synthesis. The categorization of short – medium – long refers to the research to observe the relationship between the averaged SNR and the length of the filters when orthogonal wavelets – Daubechies' wavelets, symlets, and coiflets have been used. From that research, a maximum SNR is achieved for wavelets which corresponding filter is with medium length [16]. Short filter range is 1 up to 4, medium filter range is 5 up to 12, and long filter range is which exceeds 12. For example: we need 5/7 biorthogonal with symmetric scaling filters. The 5-tap filter then can be written as a modified form which is stated by Soman, *et al.* [8]:

$$H(z) = \sqrt{2} \left(\frac{1+z}{2} \right)^2 \left(\frac{1-a}{2} z^{-1} + a + \frac{1-a}{2} z \right) \quad (9)$$

The first factor gives us two vanishing moments, while the second factor determines:

$$H(1) = \sqrt{2} \quad (10)$$

and

$$\left(\frac{1-a}{2} z^{-1} + a + \frac{1-a}{2} z \right)_{z=-1} \neq 0 \quad (11)$$

The resulting filter is a symmetric low pass filter which has 1 parameter with 5 taps.

By expanding and simplifying (11) for $H(z)$, we can get:

$$H(z) = \sqrt{2} \left(\left(\frac{1-a}{8} \right) z^{-2} + \left(\frac{1}{4} \right) z^{-1} + \left(\frac{1-a}{4} \right) + \left(\frac{1}{4} \right) z + \left(\frac{1-a}{8} \right) z^2 \right) \quad (12)$$

or

$$h = (h_{-2}, h_{-1}, h_0, h_1, h_2) = \sqrt{2} \left(\frac{1-a}{8}, \frac{1}{4}, \frac{1-a}{4}, \frac{1}{4}, \frac{1-a}{8} \right) \quad (13)$$

Meanwhile, the second filter $\bar{H}(z)$ can be stated as:

$$\bar{H}(z) = \sqrt{2} \left(\frac{1+z}{2} \right)^2 \left(b + \frac{c}{2} z + \frac{c}{2} z^{-1} + \frac{1-b-c}{2} z^2 + \frac{1-b-c}{2} z^{-2} \right) \quad (14)$$

Also, by expanding and simplifying (14) for $\bar{H}(z)$, we can get:

$$\begin{aligned} \bar{H}(z) = \sqrt{2} & \left(\left(\frac{1-b-c}{8} \right) z^{-3} + \left(\frac{2-2b-c}{8} \right) z^{-2} + \left(\frac{1+b+c}{8} \right) z^{-1} + \dots \right. \\ & \left. \dots + \left(\frac{2b+c}{4} \right) + \left(\frac{1+b+c}{8} \right) z + \left(\frac{2-2b-c}{8} \right) z^2 + \left(\frac{1-b-c}{8} \right) z^3 \right) \end{aligned} \quad (15)$$

or

$$\begin{aligned} \bar{h} &= (\bar{h}_{-3}, \bar{h}_{-2}, \bar{h}_{-1}, \bar{h}_0, \bar{h}_1, \bar{h}_2, \bar{h}_3) \\ &= \sqrt{2} \left(\frac{1-b-c}{8}, \frac{2-2b-c}{8}, \frac{1+b+c}{8}, \frac{2b+c}{4}, \frac{1+b+c}{8}, \frac{2-2b-c}{8}, \frac{1-b-c}{8} \right) \end{aligned} \quad (16)$$

Double-shift orthogonality property yields the equations below:

$$h_0 \bar{h}_3 + h_1 \bar{h}_4 + h_2 \bar{h}_5 + h_3 \bar{h}_6 = \left(\frac{1-a}{4} \times \frac{2b+c}{4} \right) + \left(\frac{1}{2} \times \frac{1+b+c}{8} \right) + \left(\frac{1+a}{2} \times \frac{2-2b-c}{8} \right) + \left(\frac{1}{2} \times \frac{1-b-c}{8} \right) = 0$$

$$\Leftrightarrow -\frac{a}{2} - b - \frac{3c}{16} + \frac{ab}{2} + \frac{ac}{4} + 1 = 0 \quad (17)$$

$$h_0 \bar{h}_5 + h_1 \bar{h}_6 = \left(\frac{1-a}{4} \times \frac{2-2b-c}{8} \right) + \left(\frac{1}{2} \times \frac{1-b-c}{8} \right) = 0$$

$$\Leftrightarrow \frac{a}{2} - ab - \frac{ac}{2} + 1 = 0 \quad (18)$$

Solutions on (16) and (17) yield:

$$b = \frac{1}{2} \left(a - 3 + \frac{6}{a} \right) \quad (19)$$

$$c = -a + 4 - \frac{4}{a} \quad (20)$$

For $a = \frac{7}{4}$, then value of $b = \frac{61}{56}$ and $c = -\frac{1}{28}$. Therefore we can determine:

$$h = (h_{-2}, h_{-1}, h_0, h_1, h_2) = \left(\frac{-3\sqrt{2}}{32}, \frac{\sqrt{2}}{4}, \frac{11\sqrt{2}}{16}, \frac{\sqrt{2}}{4}, \frac{-3\sqrt{2}}{32} \right) \quad (21)$$

22
and

$$\bar{h} = (\bar{h}_{-3}, \bar{h}_{-2}, \bar{h}_{-1}, \bar{h}_0, \bar{h}_1, \bar{h}_2, \bar{h}_3) = \left(\frac{-3\sqrt{2}}{448}, \frac{-\sqrt{2}}{56}, \frac{115\sqrt{2}}{448}, \frac{15\sqrt{2}}{28}, \frac{115\sqrt{2}}{448}, \frac{-\sqrt{2}}{56}, \frac{-3\sqrt{2}}{448} \right) \quad (22)$$

It can be shown that the normality condition is satisfied. That is, it can be seen, with no shift, multiplying the filter coefficients in corresponding position, and then summing all multiplied coefficients, the result is 1. This result can be explained easily in figure 4.

0	$\frac{-3\sqrt{2}}{32}$	$\frac{\sqrt{2}}{4}$	$\frac{11\sqrt{2}}{16}$	$\frac{\sqrt{2}}{4}$	$\frac{-3\sqrt{2}}{32}$	0
$\frac{-3\sqrt{2}}{448}$	$\frac{-\sqrt{2}}{56}$	$\frac{115\sqrt{2}}{448}$	$\frac{15\sqrt{2}}{28}$	$\frac{115\sqrt{2}}{448}$	$\frac{-\sqrt{2}}{56}$	$\frac{-3\sqrt{2}}{448}$

Figure 4. Filters coefficient of 5/7 Biorthogonal

Applying the cascade algorithm up to 20 iteration to form both scaling and wavelet functions for decomposition can be shown in figure 5. From this figure, we can see visually that (a) we can construct plots of both scaling and wavelet function for decomposition using successive approximations (or Cascade Algorithm) from 1 to 20 iterations. After 20 iterations applied, we can get smooth functions graphics, or we can say, after 20 iterations, both scaling and wavelet functions converge to fixed points; (b) biorthogonal wavelet bases maintain the symmetrical property both for wavelets and scaling functions by relaxing the orthogonality constraint.

Meanwhile, Applying the cascade algorithm up to 20 iteration to form both scaling and wavelet functions for reconstruction can be shown in figure 6. Two conclusions on constructing both scaling and wavelet functions for decomposition, also concluded similarly when it is applied for reconstruction process, i.e. graphics displayed more smooth after 20 iterations and that we get the symmetrical wavelet and scaling functions after 20 iterations too.

4.1 Image Reconstruction Tests using MSE and Euclidean Distance

From the wavelet design previously, we have constructed a 5/7 biorthogonal, where 5 (five) indicates the length of decomposition filter, that is $N_d = 5$, while 7 (seven) indicates the length of reconstruction filter, that is $N_r = 7$.

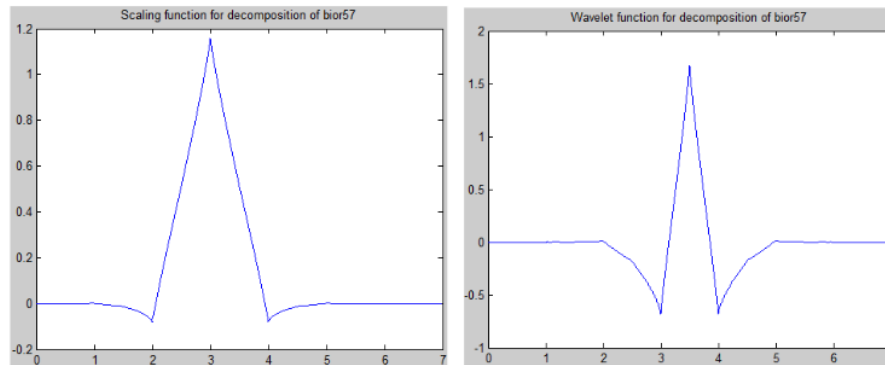


Figure 5. Scaling (left) and wavelet (right) functions of 5/7 biorthogonal filters for decomposition.

Then, orthogonal/biorthogonal wavelet types, i.e. Haar, db5, coif3, sym4, and bior2.4 which used in former research together with the new wavelet designed were tested. Some test was conducted to measure the performance based on mean-squared error (MSE) between reconstructed images of decomposed iris images and their original input images. In these tests, an unwrapped iris image from CASIA database, as well as from an image captured by Irdosoft 3.8 camera, as we can see in figure 7.

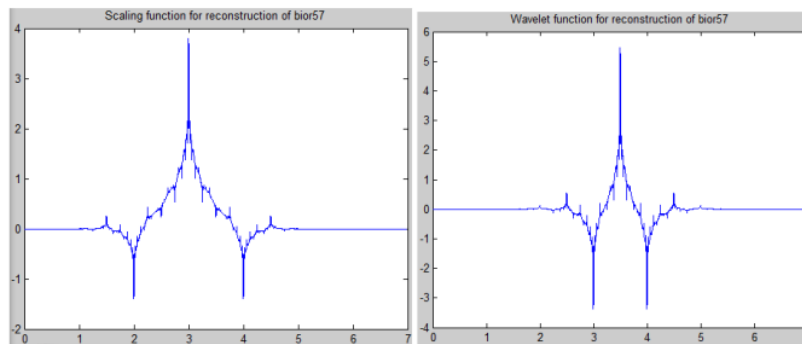
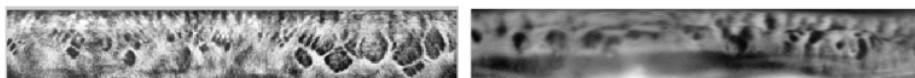


Figure 6. Scaling (left) and wavelet (right) functions of 5/7 biorthogonal filters for reconstruction.



(a) example of CASIA image

(b) example of iris captured by Irdosoft 4.0 camera

Figure 7. Example of iris images for Euclidean distance and MSE tests

Table 1 shows the results of Euclidean distance and MSE tests between reconstructed images and its original images which are shown in figure 7.

Table 1. Euclidean distance and MSE between reconstructed images and the original images.

No.	Wavelet types	CASIA database image		Image captured by Irdosoft 3.8	
		Euclidean distance	MSE	Euclidean distance	MSE
1	Haar	$1,1567 \times 10^{-13}$	$9,5565 \times 10^{-28}$	$9,5329 \times 10^{-14}$	$8,2615 \times 10^{-28}$
2	db5	$1,0832 \times 10^{-10}$	$8,3811 \times 10^{-22}$	$9,7398 \times 10^{-11}$	$8,6239 \times 10^{-22}$
3	coif3	$7,1285 \times 10^{-11}$	$3,6297 \times 10^{-22}$	$5,7406 \times 10^{-11}$	$2,9959 \times 10^{-22}$
4	sym4	$5,8662 \times 10^{-11}$	$2,4580 \times 10^{-22}$	$4,2551 \times 10^{-11}$	$1,6460 \times 10^{-22}$
5	bior2.4	$6,0709 \times 10^{-14}$	$2,6325 \times 10^{-28}$	$6,5122 \times 10^{-14}$	$3,8554 \times 10^{-28}$
6	bior5.7	$7,1054 \times 10^{-14}$	$5,0487 \times 10^{-28}$	$4,9228 \times 10^{-14}$	$2,2031 \times 10^{-28}$

^{a)} new 5/7 biorthogonal wavelet

As we can see in Table 1, the new 5/7 biorthogonal wavelet (bior5.7) has the best result in reconstructing the decomposed image which is captured by Irdosoft 3.8 camera, when compared with other types of wavelet (Haar, db5, coif3, sym4, and bior2.4). We can notice this best result in two measures, i.e Euclidean distance as well as MSE, applying bior5.7 give us minimum Euclidean Distance and also minimum MSE. However, if applied to CASIA database image, bior5.7 give the good result compared with 4 (four) type of wavelets (Haar, db5, coif3, and sym4), although it only differs slightly below the bior2.4 which results in best performance, regarding in Euclidean distance and MSE.

5. Conclusion

From developing new wavelet, step-by-step until getting the results, it can be obtained some conclusions below.

1. A new type of wavelet has been found, i.e. bior5.7, which has properties: biorthogonal; filter length for decomposition and reconstruction, respectively, are $N_d = 5$ and $N_r = 7$.
2. The new 5/7 biorthogonal wavelet (bior5.7) has the best result in reconstructing the decomposed image which is captured by Irdosoft 3.8 camera, when compared with other types of wavelet (Haar, db5, coif3, sym4, and bior2.4). This can be seen in two measures, i.e Euclidean distance as well as MSE, applying bior5.7 give us minimum Euclidean Distance ($4,9228 \times 10^{-14}$) and also minimum MSE ($2,2031 \times 10^{-28}$).
3. When applied to CASIA database image, bior5.7 give the good result compared with 4 (four) type of wavelets (Haar, db5, coif3, and sym4), although it only differs slightly below the bior2.4 which results in best performance, regarding in Euclidean distance and MSE.

5.1 Recommendation and comments

From the research results, we would like recommend as well as giving comments as the herebelows.

1. For improving this manuscript in advance, the research can be continued to observe other wavelets and/or construct other type of wavelets, for which we can get the best-matched wavelet for iris extraction.
2. The new wavelet is expected to be used and to be a reference to next researchers that will explore the iris feature extraction for which the high rate of recognition can be achieved.
3. This research is highly expected to provide more detailed description on designing step to new wavelet which is matched for iris images. Furthermore, it can triggers other researchers to develop

the new wavelets for different biometrics systems, i.e. fingerprints, face, palmprint, and dynamic signatures.

References

- [1] CASIA-IrisV1, <http://biometrics.idealtest.org/>
- [2] Isnanto, R.R., T.S. Widodo, Suhardjo, and A. Susanto, 2012, "Increased Iris Recognition Rate by Observing Wavelet Decomposition Levels and Number of Images Stored", *Journal of Information and Communication Technologies (JICT)*, ISSN: 2047-3168, Vol. 2 Issue 5, 2012, pp. 1-7.
- [3] Kusuma A A, "Pengenalan Iris Mata Menggunakan Pencirian Matriks Ko-Okurensi Aras Keabuan", Skripsi S-1, Universitas Diponegoro, Semarang, 2009.
- [4] Misiti M, Misiti Y, Oppenheim G, and Poggi J M, *Wavelet Toolbox For Use with Matlab*, User's Guide Version 3, The Math Works, Natick, MA, 2004.
- [5] Mustofa, A., 2007, "Sistem Pengenalan Penutur dengan Metode Mel-Frequency Wrapping", *Jurnal Teknik Elektro*, vol 7, No.2, September 2007, pp. 88-96.
- [6] Wijayanto W S, *Identifikasi Iris Mata dengan Tapis Gabor Wavelet dan Jaringan Syaraf Tiruan Learning Vector Quantization (LVQ)*, Diponegoro University, Semarang, 2005.
- [7] Burrus C S, Gopinath R A, and Guo H, 1998, *Introduction to Wavelets and Wavelet Transforms: a Primer*, Prentice-Hall, Upper Saddle River, New Jersey.
- [8] Soman, K P, Ramachandran K I, and Resmi N G, 2010, *Inside into Wavelets: From Theory to Practice*, 3rd edition, PHI Learning Private Limited, New Delhi.
- [9] Isnanto R R, Widodo T S, Suhardjo, and Susanto A, 2012, "Comparison Analysis on Recognition Rate of Iris using Haar and Daubechies Wavelet Tranforms", *International Journal of Information Technology and Network Application (IJITNA)*, ISSN: 2168-2178, Vol. 2 No. 1, pp. 21-27.
- [10] Isnanto R R, Widodo T S, Suhardjo, and Susanto A, 2012, "Wavelet Types Comparison for Extracting Iris Features Based on Energy Compaction", *Proceedings of The 3rd ICSIT 2012 (International Conference on Soft Computing, Intelligent System, and Information Technology)*, ISBN: 978-602-97124-1-4, Bali, pp. 88-93.
- [11] Isnanto R R, Widodo T S, Suhardjo, and Susanto A, 2012, "Comparison Analysis on Recognition Rate of Iris using Haar and Symlet Wavelet Tranforms", *Proceedings of The 13th Seminar on Intelligent Technology and Its Applications, SITIA 2012*, ISSN: 2252-8296, Surabaya, pp. 1-6.
- [12] Mallat S, 1999, *A Wavelet Tour of Signal Processing*, 2nd edition, Academic Press, London.
- [13] Strang G and Nguyen T, 1996, *Wavelets and Filter Banks*, Wellesley-Cambridge Press, Wellesley, MA.
- [14] Qi, X, 2003, "Object Contour Matching Using the Biorthogonal Wavelet Transform", *Proc. of the 5th International Conference on Computer Vision, Pattern Recognition, and Image Processing (CVPRIP'03)*, pp. 668-671, Cary, North Carolina, September 26-30, 2003
- [15] Isnanto R R, 2012, *Texture-based Feature Extraction on Iris Image using Wavelets Transform*, Electrical Engineering and Information Technology Department, Faculty of Engineering, Gadjah Mada University, Indonesia.
- [16] Nikolaev N and Gotchev A, 2000, "ECG Signal Denoising Using Wavelet Domain Wiener Filtering", *Proceeding of the European Association for Signal and Image Processing (EURASIP)*.

Acknowledgments

Authors wishing to acknowledge assistance or encouragement from colleagues, they are: Mr. Rukun Santoso and Mr. Achmad Hidayatno who had gives some interesting views for insight understanding into wavelets. Also, authors have to thank to BOPTN FT Undip for their financial support for which this research can be done.

Constructing New Biorthogonal Wavelet Type which Matched for Extracting the Iris Image Features

ORIGINALITY REPORT

19%

SIMILARITY INDEX

14%

INTERNET SOURCES

9%

PUBLICATIONS

5%

STUDENT PAPERS

PRIMARY SOURCES

1	www.ukessays.com Internet Source	2%
2	eprints.undip.ac.id Internet Source	2%
3	fr.slideshare.net Internet Source	1%
4	Submitted to (school name not available) Student Paper	1%
5	Bao Wang, Xiang-Ke Chang, Xiao-Lu Yue. "A generalization of Laurent biorthogonal polynomials and related integrable lattices", Journal of Physics A: Mathematical and Theoretical, 2022 Publication	1%
6	T. Arathi, K. P. Soman, Latha Parameshwaran. "Chapter 118 Spline Biorthogonal Wavelet Design", Springer Science and Business Media LLC, 2010 Publication	1%

7	zenodo.org Internet Source	1 %
8	ebin.pub Internet Source	1 %
9	Shui-Hua Wang, Yu-Dong Zhang, Zhengchao Dong, Preetha Phillips. "Pathological Brain Detection", Springer Science and Business Media LLC, 2018 Publication	1 %
10	electroinf.uoradea.ro Internet Source	1 %
11	en.wikipedia.org Internet Source	1 %
12	Submitted to Jaypee University of Information Technology Student Paper	1 %
13	ce.et.tudelft.nl Internet Source	<1 %
14	Y.-J. CHEN, S. H. DAVIS. "Directional solidification of a binary alloy into a cellular convective flow: localized morphologies", Journal of Fluid Mechanics, 1999 Publication	<1 %
15	www.scribd.com Internet Source	<1 %

16

inside.mines.edu

Internet Source

<1 %

17

Aparna Vyas, Soohwan Yu, Joonki Paik.
"Multiscale Transforms with Application to
Image Processing", Springer Science and
Business Media LLC, 2018

Publication

<1 %

18

K Shivith, K Rameshkumar. "AE signature
analysis using continuous and discrete
wavelet transforms to predict grinding wheel
conditions", IOP Conference Series: Materials
Science and Engineering, 2021

Publication

<1 %

19

"Multiscale Signal Analysis and Modeling",
Springer Science and Business Media LLC,
2013

Publication

<1 %

20

[Submitted to The University of Buckingham](#)

Student Paper

<1 %

21

www.uta.edu

Internet Source

<1 %

22

cam.mathlab.stthomas.edu

Internet Source

<1 %

23

aftre.nssga.org

Internet Source

<1 %

autodocbox.com

24

Internet Source

<1 %

25

dokumen.tips

Internet Source

<1 %

26

link.springer.com

Internet Source

<1 %

27

www.sparrho.com

Internet Source

<1 %

28

repository.unusa.ac.id

Internet Source

<1 %

29

repozitorij.unizg.hr

Internet Source

<1 %

30

www.researchgate.net

Internet Source

<1 %

31

S A Hashim, S Daliman, I N Md Rodi, N Abd Aziz, N A Amaludin, A Eh Rak. "Analysis of Oil Palm Tree Recognition using Drone-Based Remote Sensing Images", IOP Conference Series: Earth and Environmental Science, 2020

Publication

<1 %

32

Y. Mallet, O. de Vel, D. Coomans.
"Fundamentals of Wavelet Transforms",
Elsevier BV, 2000

Publication

<1 %

Exclude quotes Off

Exclude matches Off

Exclude bibliography On